Communications to SIMAI Congress,
ISSN 1827-9015, Vol. 3 (2009) 281 (12pp)
DOI: 10.1685/CSC09281

A tool for multi-platform remote sensing processing

Gaetana Ganci [12], Ciro Del Negro [1], Luigi Fortuna [2], Annamaria Vicari [1]

[1] *Istituto Nazionale di Geofisica e Vulcanologia*
Sezione di Catania, Italy
ganci@ct.ingv.it
delnegro@ct.ingv.it
vicari@ct.ingv.it

[2] *Dipartimento di Ingegneria Elettrica Elettronica e dei Sistemi,Facoltà di Ingegneria*
Università degli Studi di Catania, Italy
lfortuna@diees.unict.it

Abstract

Thermal remote sensing of volcanic activity can be efficiently dealt with by observations carried out at high repetition rates by high spectral resolution radiometers, much more than by observations carried out at high geometrical resolutions. This held true for radiometers AVHRR (in spite of the small dynamic range of channels, mainly MIR, unsuited to volcano observation) and MODIS, and was recently demonstrated to hold true also for SEVIRI, onboard the geosynchronous platforms MSG1 and MSG2. A digital image processing tool in near-real-time of thermal infrared satellite data acquired by MODIS and AVHRR sensors (low temporal resolution) has been successfully experimented on Etna volcano. This multi-approach method was integrated with the information coming from SEVIRI sensor that allows to obtain a high temporal resolution. We conducted a preliminary study to verify the applicability of the SEVIRI as an instrument suitable to be employed in an operational system of early hot spot detection. This multi-platform system has been validated and tested on the Mt Etna 2008 eruption.

Keywords: `remote sensing, multi-platform, Etna volcano`

1. Introduction

Over the last 20 years, multispectral infrared (IR) observations carried out for by the spacecrafts have shown that spaceborne remote sensing of high-temperature volcanic features is feasible and robust enough to turn into volcano monitoring. High-spatial, low-temporal resolution data (16 days) from the Landsat thematic mapper were firstly used by Francis and McAllister [3] to detect radiance emitted by a lava dome in Lascar

Received 13/02/2009, in final form 15/07/2009
Published 31/07/2009

Volcano (Chile). Successively the potential of such data was also extended to the thermal analysis of active lava flows, lava domes, lava lakes and fumaroles field. Although high-spatial resolution imagery (e.g. 30 to 120 m pixels) can yield useful information regarding the detailed thermal properties of volcanic feature, the low spatial but high temporal resolution of meteorological satellites has proven ideal for continuous monitoring of volcanic activity. Despite of the fact that the volcanic features of interest are usually much smaller than the nominal pixel size of the sensors, meteorological satellites, such as the Advanced Very High Resolution Radiometer, the MODerate Resolution Imaging Spectro-radiometer and even the Spinning Enhanced Visible and Infrared Imager, can detect emitted radiance in the shortwave infrared (SWIR) part of the electromagnetic spectrum, a region in which active lava flows, vents and domes emit copious amounts of energy.

The AVHRR instruments onboard the National Oceanic and Atmospheric Administration (NOAA) polar-orbiting satellites, provide data at least 4 times a day for any subaerial volcano with a spatial resolution of about 1 km. Nowadays AVHRR data are employed for volcanic purposes both for thermal anomalies detection [4] for ash clouds monitoring [7].

The sun-synchronous Moderate Resolution Imaging Spectrometer (MODIS) offers an additional data set to look at volcanic hot spots. The advantages of using MODIS data are the up to 10 wavebands suitable for hot-spot detection. In particular band 21, also known as the "fire channel", was designed to have a much higher saturation temperature of about 500 K. For these reasons MODIS data were supported as basis for automated systems to detect and monitor volcanic eruptions for the entire globe [9].

The launch of MSG SEVIRI on August 2002 provides a unique opportunity for a volcanic eruption detection system in real-time by providing images at 15 minutes interval. In spite of the low spatial resolution, the frequency of observations afforded by the MSG SEVIRI was recently applied both for fire detection [6] and for the monitoring of effusive volcanoes in Europe and Africa [5].

If near-real-time volcano monitoring is to be achieved using satellite data, images must be routinely received and analyzed rapidly. To this end, we have developed a multi-platform tool for satellite image analysis and volcanic processes characterization. Computing routines were designed to allow for the joint exploitation of radiometers AVHRR, MODIS and SEVIRI in operational monitoring, in response to the need for fast and robust determination of hot spot detection at active volcanoes. In this paper we illustrate the theoretical background for remote sensing and image satellite analysis and how some of the well known algorithms for cloud detection

DOI: 10.1685/CSC09281

and hotspot detection were implemented in our tool. Code efficiency and reliability of results were tested and demonstrated during the Etna 2008 ongoing eruption.

2. Remote Sensing Methodologies

Infrared remote sensing is based on the simple principle that everything above absolute zero emits radiation in the infrared range of the electromagnetic spectrum and that how much energy is radiated, and at which wavelengths, depends on the emissivity of the surface and on its kinetic temperature. The emission pattern/spectra of the electromagnetic spectrum of a blackbody are determined by Planck's law as a function of its wavelength and temperature:

$$R_\lambda(T) = \frac{2hc^2}{\lambda^5 \left(e^{\frac{hc}{\lambda k T}} - 1\right)}$$

Where R_λ is the radiance emitted at the wavelength λ, h is the Plank constant $[6.63 \cdot 10^{-34} JHz^{-1}]$, c is the speed of light $(3 \cdot 10^8 ms^{-1})$, k the Boltzmann constant $[1.38 \cdot 10^{-23} JK^{-1}]$ and T the temperature $[K]$.

If we can measure the part of the spectral radiance, R_λ, which was radiated thermally from the surface, then we can use Planck's formula to derive the kinetic temperature, T, of the surface thus:

$$T = \frac{hc}{\lambda k} \cdot \frac{1}{\ln\left(1 - \frac{2hc^2}{\lambda^5 R_\lambda}\right)}$$

These relationships enhance the crucial role of the wavelength λ in the computation of the emitted radiance. Moreover it's important to stress how the dominant wavelength ($\lambda_{\max}$) provides valuable information about which part of the thermal spectrum we might want to sense in.

Indeed the bands in the short wavelength infrared (SWIR) part of spectrum are particularly suitable for monitoring of thermal anomalies associated with the volcano activity (hot spot detection). This can be explained with the help of Wien's displacement law, which states an inverse relationship between the temperature of a black body and wavelength at which it has its peak emission. According to the Wien's displacement law the hotter a surface is, the peak of its temperature curve shifts to the shorter wavelengths, and the colder a surface is, its peak temperature shifts to the longer wavelengths.

$$\lambda_{MAX}(\mu m) = \frac{2898}{T(K)}$$

Fig. 1 shows a graph of the energy emitted at a range of electromagnetic wavelengths by a black body at different temperatures. It is worth noting that the energy emitted by an object increases by several orders of magnitude with temperature in the $3 - 4\mu m$ region. At longer wavelengths, such as $11\mu m$, there is a much reduced increase in emitted energy per degree of temperature increase.

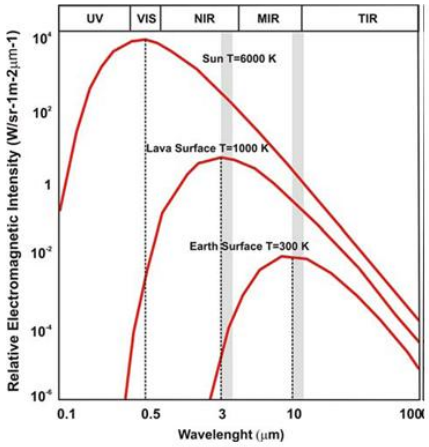

Fig. 1. Spectral wavelength versus emitted radiance (as intensity) from thermal radiators at three temperatures ranging from that of the sun to the earth's surface.

All the satellites we refer in this work detect radiance in spectral wavebands centered at 4 and $11 - 12\mu m$. These wavebands coincide with the wavelengths of peak emission for high-temperature volcanic heat sources and ambient earth surface temperatures respectively. Thus, they are useful channels for hot spot detection [9].

If the radiant source occupies less than a whole pixel, as is the case for fumaroles, a small incandescent vent or a crusted lava surface with incandescent cracks, then the pixel-integrated temperature is less than the actual surface temperature of the hot areas. Furthermore, the temperature appears lower at longer wavelengths. By determining pixel-integrated temperature in two spectral bands we can estimate both the temperature and size of hot areas that occupy less than a complete pixel.Moreover it was demontrated [9] that although the presence of a sub-pixel-sized hot spot causes emission at $11\mu m$ to increase by only 1%, the presence of the same feature causes emission at $4\mu m$ to increase by more than 200%. Remotely sensed infrared data, therefore, provide a tool that is well suited to identify volcanic hotspots at the pixel or sub-pixel scale.

DOI: 10.1685/CSC09281

3. Multi-Platform Remote Sensing

Satellites may be broadly divided into geostationary satellites and polar orbiting satellites with respect to the overpasses and orbital characteristics. Geostationary satellites, such as MSG SEVIRI, provide high temporal resolution (15 minutes) and keep fixed the view angle. So they are very useful to give very important information about phenomena which change continuously such as dynamic volcanic activities. Polar orbiting satellites instead, such as MODIS and AVHRR have a lower temporal resolution: MODIS gives four images for a particular location per day, which in case of AVHRR are 2 images per day. However these satellites include larger areas of the earth than the geostationary, even if they change their position with respect to Earth and hence the view angle. Furthermore, operating from a lower altitude (800 km vs 36000 km), their spatial resolution is much higher than the geostationary (1 km for AVHRR and MODIS vs 4 km for SEVIRI). MSG SEVIRI, AVHRR and MODIS have some benefits and limitations in volcano monitoring and it would be really useful to combine both the benefits of the geostationary satellites and polar orbiting satellites by combining their strengths.

The multi-platform remote sensing tool is basically composed by three packages: Pre-processing, Product Generation and Post-processing. Each package consists of several independent executable modules. The modules of Pre-processing are necessary for initial geolocation and calibration, the modules of Product Generation compute higher-level products from the satellite band data and the ones of Post-processing project raw geometry data to a cartographic reference system and export the derived image files to standard DTP formats (bmp, jpeg, gif, etc.). The entire package is controlled by a Control Unit and the user can configure these settings.

As for the first package, it involves preprocessing of the images. This consists of a sequence of operations, including image registration, geometric correction and resizing. Different strategies are applied for preprocessing different sensor data. Polar-orbiting satellites such as MODIS and AVHRR need special procedures for georeferencing the images, unlike the geostationary SEVIRI.

Finally, the product generation block includes the atmospheric correction, the cloud mask and the hotspot detection. To avoid technical details, the atmospheric correction won't be addressed, while we'll focus on the algorithms for cloud mask and hotspot.

3.1. *Cloud Mask*

The cloud mask is a matrix where every pixel is classified as cloud or not, with a level of confidence. Clouds are the dominant factor of the radiation budget of the earth atmosphere. As mentioned in Hartmann et al 1992 the radiation budget of clouds depends considerably on their type: high thin clouds tend to have a warming effect, while low clouds have a cooling effect.

Even in this case the approaches vary according to the sensor. Firstly a land mask is needed. The procedure for AVHRR is based on a threshold method. We fix four conceptual domains (sea, land, night and day) and empirically found the best value and range of confidence for our longitudes. Moreover by these tests we can distinguish between medium-high clouds, cirrus or semi-transparent clouds.

As for MODIS images, we used the algorithm proposed by the MODIS Cloud Mask Team [1]. This run by using a series of spectral tests that rely on radiance (temperature) thresholds in the infrared and reflectance thresholds in the visible to determine the likelihood of a pixel being cloud contaminated. The final cloud mask quantifies our level of confidence for each pixel: clear, probably clear, uncertain, and cloudy. After that, the algorithm for hot spot detection is launched if the image is determined to be clear of cloud. Fig. 2 illustrate an example of cloud mask. The short

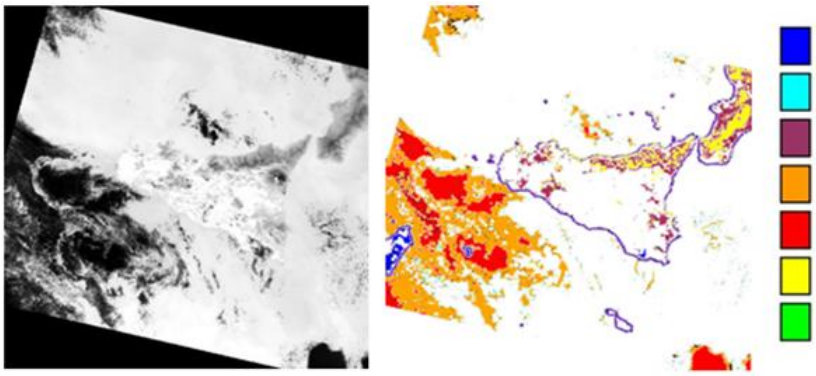

Fig. 2. MODIS Cloud Mask.

interval of 15 minutes between images is capitalized, as for SEVIRI images, for clouds individuation. Indeed we implemented the algorithm proposed by de Ruyter de Wildt [2] that extends traditional spectral classification with a detection of changes between images. This improves the detection of clouds in instantaneous images, because these often change more in time than the surface. For daily data is required a test based on the reflectance

DOI: 10.1685/CSC09281

value. We compute the reflectance (r) from the radiance (R_λ) according to:

$$r = \frac{\pi R_\lambda d(t)_S^2 A}{R_{TOA} \cos\theta(t,x)}$$

where $d(t)_S A$ is the distance earth-sun in AU at time t, $R_{TOA}$is the solar irradiance at 1 AU in $mWm^{-2}(cm^{-1})^{-1}$and θ is the solar zenith angle at time t and location x.

Fig. 3 shows an example of cloud mask: in this case only the presence of cloud or not is distinguished, so the output will be a true/false matrix. All the implemented algorithms rely on simple threshold tests and, except from the one for SEVIRI, open questions arise from the right choice of the thresholds being necessary dependent by the latitude, the season and the time of the day. More sophisticated solutions are required in order to find a generalized product.

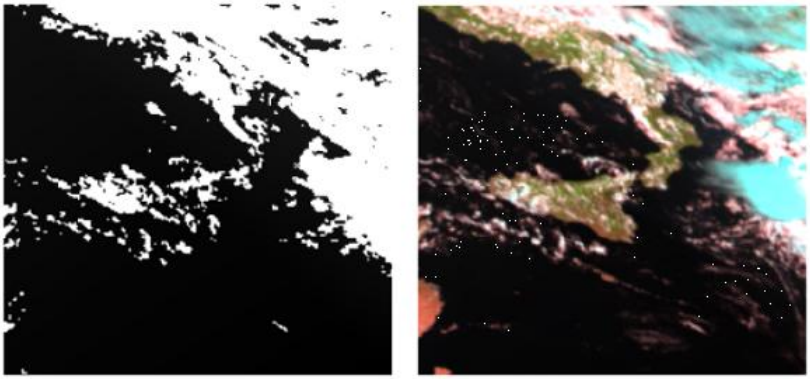

Fig. 3. SEVIRI Cloud Mask.

3.2. *Hot Spot Detection*

The automatic detection of hotspots is a nontrivial question since an appropriate threshold radiance value must be chosen to distinguish those pixels that contain hotspots from those that do not. Techniques for automatically detecting hotspots in satellite data generally rely on two distinct methods: (i) the spectral comparison and (ii) the spatial comparison. The spectral method is based on the fact that $4\mu m$ and $11 - 12\mu m$ brightness temperatures should be very similar for surfaces at ambient temperature. Instead in presence of a high-temperature radiator this difference varies largely since the $4\mu m$ brightness temperature increases dramatically when compared to the $11\mu m$ brightness temperature recorded for the same pixel. This method is fairly robust since it automatically accommodates changes

in the ambient background temperature and solar heating effects. The spatial method assumes that the $4\mu m$ brightness temperature of a hotspot pixel will be significantly different to that of neighboring background pixels. By assuming that each pixel in an image is a "potential" hotspot and statistically comparing its $4\mu m$ brightness temperature to that of its neighbors, positive discrimination of hotspots can be achieved when the temperature difference exceeds a certain threshold. Sometimes called the "contextual approach" it accommodates the influence of seasonal and geographical effects on the $4\mu m$ signal by tailoring the threshold for positive detection to the prevailing local background.

Hotspot detection for AVHRR images was performed up taking both the spectral and spatial comparison methods. In particular we compute the temperature difference between channel 3 and 4 and evaluate if it exceeds a varying threshold. The threshold is chosen making use of the spatial comparison method. As for MODIS images, we implemented the contextual approach of Harris et al [4]. This technique uses the difference between brightness temperature in channel 21 (or 22) and channel 31 (ΔT) and sets a ΔT threshold obtained from within the image, to define whether a pixel is hot. Due to the low $NE\Delta T$ of channel 22, we use channel 22 data if they are unsaturated. If channel 22 is saturated, we use channel 21. The algorithm first defines a "nonvolcanic" portion of the image and uses the maximum ΔT from that portion to set a threshold. Pixels belonging to the volcanic area are then scanned and all the pixels that are greater than the threshold are classified as hot. An example of the hot spot detection results is given in fig. 4, where the observed flow field is superimposed to satellite image of 22 July showing good correspondence between the pixels flagged as hot and the actual lava extent [8]. The same procedure was applied to SEVIRI data channel 4 and 9. A hotspot image during 15 May 2008 is showed in fig. 5.

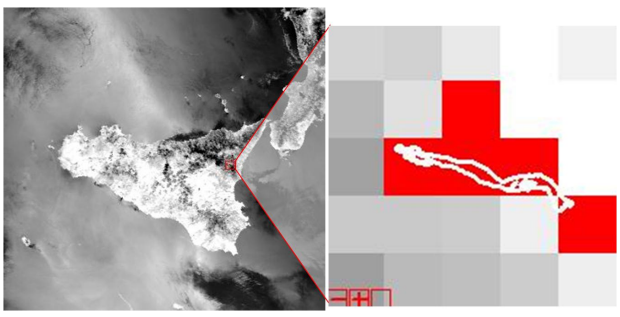

Fig. 4. MODIS Hotspot.

DOI: 10.1685/CSC09281

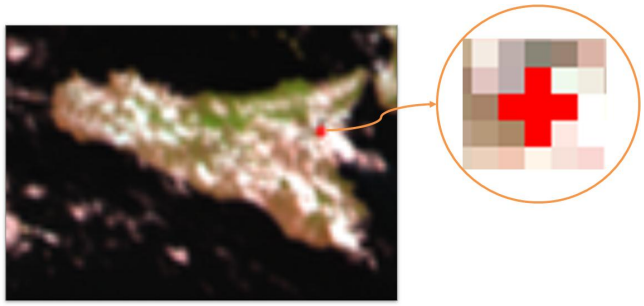

Fig. 5. SEVIRI Hotspot.

4. A study case: Etna 2008 eruption

Etna's 2008 eruption provided the opportunity to verify our model's ability to monitor the thermal state of the volcano characterized by different phases of activity form strombolian activity to lava fountain and lava flows.

On the afternoon of 10 May 2008, a powerful eruptive paroxysm, lasted about 4 hours, preceded the new eruption started on the morning of 13 May 2008 and still going on. After a seismic swarm of more than 200 earthquakes and significant ground deformation, a fissure erupted in the summit area immediately to the east of Etna's summit craters. On the afternoon of the same day, a new eruptive fissure opened with a number of vents displaying Strombolian activity and emission of lava flows toward the Valle del Bove (a wide depression that cuts the eastern flank of the volcanic edifice). An helicopter survey carried out on 14 May at 13:00 showed the two eruptive fissures: a first one opened on the east of the summit craters (3000 m asl) spreading along North-South direction and a second fissure started from the east flank of South-East Crater summit cone of Mt Etna (2900-2500 m asl) spreading with ENE-WSW orientation toward the Valle del Bove. During the following 24 hours the lava traveled approximately 6 km to the east, but thereafter its advance slowed and stopped. The most distant lava fronts stagnating about 3 km from the nearest village, Milo. Between 16 and 18 May ash emissions became more frequent and produced small but spectacular clouds, whereas the rate of lava emission showed a gradual diminution. During late May and the first week of June, the activity continued at low levels, with lava flows advancing only a few hundred meters from the vents as of 4 June. Four days later, on 8 June, there was a considerable increase in the vigor of Strombolian activity and lava output rate. During the following weeks, lava flows advanced up to 5 km from the source vents. Volcanic thermal anomalies have been observed almost continuously over the same Mt Etna flank in accordance with the occurrence of the lava effusion. A signif-

icant increase in the number of hotspots detected, with an evident increase even in their relative intensity, was instead recognized in the late evening of 13 May in accordance with the opening of the new eruptive fissure on NE side of SE Crater. Starting from 14 May several hotspots of high intensity have been flagged over the target area, indicating the clear presence of a lava flow.

Figures 6 and 7 [8] show the number of thermal anomalies observed in the volcanic edifice (inside a $25km^2$ box centered in the summit craters) in a period from 1 to 31 May, for SEVIRI and MODIS and AVHRR respectively. The number of pixels classified as hot for SEVIRI data is normalized with respect to the total number of images available per day (nominally 96). It's worth noting as the number of thermal anomalies follows the fluctuation of eruptive activity. In particular, the strongest eruptive phase observed during 15 May is confirmed by all the satellite datasets with the maximum value of hotspots. The same behavior is pointed out for the minor or stationary activity during the last days in May characterized by strombolian activity. Although AVHRR, MODIS and SEVIRI hotspots were obtained processing different datasets and with different procedures, they are highly correlated. This states the robustness and reliability for the methodology since it is independent of the satellite system and sensors.

It's worth noting as the SEVIRI data show a daily hotspot during 10 May stating the detection of the paroxysm, while the other two sensors didn't identify anything probably due to the cloud coverage and to their lower temporal resolution. A slight discrepancy between MODIS and AVHRR should be interpreted in term of: i) better temporal coverage for AVHRR sensor both for temporal resolution and for historical dataset; ii) residual effects due to the re-sampling of AVHRR data. However the multi sensor approach allows monitoring to be complete and continuous employing the synergy of the observations.

5. Conclusions

A tool for multi-platform remote sensing has been presented. This tool is designed for an operational pre-, product- and post-processing of dataset acquired by AVHRR, MODIS and SEVIRI sensors. Currently, the product package consists of three cloud mask algorithms one for each sensor and algorithms for hotspot detection based both on a threshold method and on a contextual approach. The ultimate goal of this work is to provide an instrument to automatic monitor the thermal state of active volcanoes with a refresh time of 15 minutes. Preliminary results on the Etna 2008 ongoing eruption strongly encourage us to improve this instrument. All the

DOI: 10.1685/CSC09281

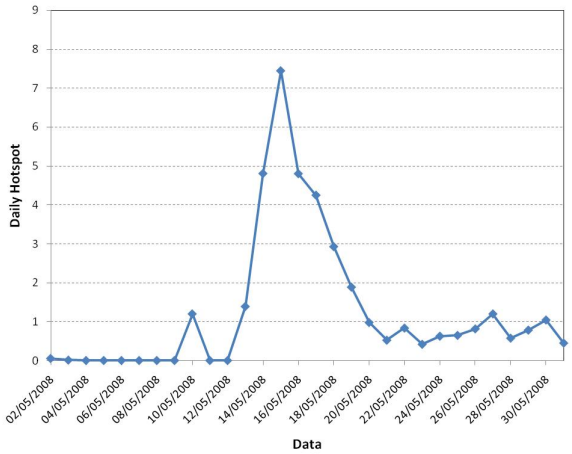

Fig. 6. Daily hotspots detected from SEVIRI data during 1 to 31 May 2008. The number of hotspot is normalized with respect to the total number of images per day.

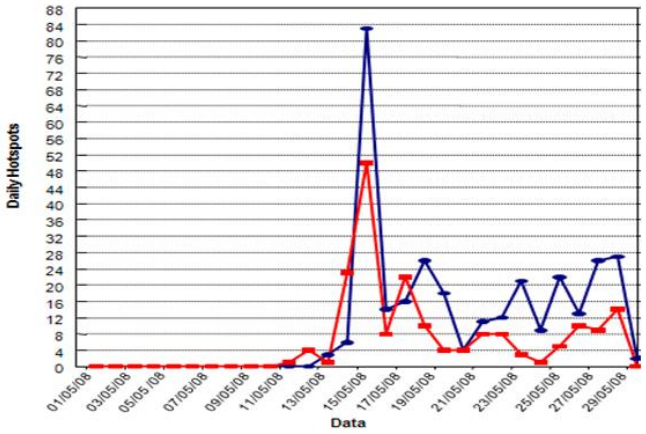

Fig. 7. Daily Hotspot for AVHRR data (red dotted line) and MODIS data (blue dotted line) during 1 to 31 May 2008.

satellites data show indeed the same temporal behavior following the different phases of the eruption. Moreover, thanks to SEVIRI data, it's possible to observe short dynamic activities such as the paroxysm preceding the eruption. Anyway additional products will be available in the near future. Thereby, the modular architecture ensures a straightforward integration for own and third party algorithms because new modules have to be registered only within the Control Unit module.

Acknowledgements

This study was undertaken with financial support from the V3-LAVA project (DPC-INGV 2007-2009 contract). This work was developed in the frame of the TecnoLab, the Laboratory for the Technological Advance in Volcano Geophysics organized by DIEES-UNICT and INGV-CT.

REFERENCES

1. S. Ackerman, K. Strabala,P. Menzel,R. Frey, C. Moeller, L. Gumley, et al. , Discriminating Clear-Sky From Cloud With MODIS, Algorithm Theoritical Basis Document (MOD35),(2002), NASA Goddard Space Flight Center
2. M. S. De Ruyter de Wildt, G. Seiz and A. Grn, Operational snow mapping using multitemporal Meteosat SEVIRI imagery. *Remote Sensing of Environment*,(2007), doi:10.1016/j.rse.2006.12.008
3. P. W. Francis, R. McAllister, Volcanology from space; using Landsat thematic mapper data in the Central Andes. *Eos, Transactions of the American Geophysical Union*,**67**,(1986), 170-171
4. A. J. L. Harris, S. E. J. Swabey and J. Higgins, Automated threshold of active lavas using AVHRR data, *Int. J. Remote Sensing*,textbf16,(1995), pp. 3681-3686.
5. B. Hirn,C. Di Bartola,G. Laneve,E. Cadau and F. Ferrucci, Seviri onboard Meteosat Second Generation, and the quantitative monitoring of effusive volcanoes in Europe and Africa 2008 *IEEE International Geoscience & Remote Sensing Symposium July 6-11*,(2008),Boston, Massachusetts, U.S.A.
6. G. Laneve, E. G. Cadau, Quality assessment of the fire hazard forecast based on a fire potential index for the Mediterranean area by using a MSG/SEVIRI based fire detection system,*Geoscience and Remote Sensing Symposium, IGARSS*,(2007), doi 10.1109/IGARSS.2007.4423337, pp 2447-2450
7. N. Pergola and V. Tramutoli, Two years of operational use of SANA (Sub-pixel Automatic Navigation of AVHRR) scheme: accuracy assessment and validation,*Rem. Sens. Environ.*, **82**, no.2, (2003), pp 190-203
8. A. Vicari, G. Ganci, A. Ciraudo, A. Herault, I. Corviello, T. Lacava, F. Marchese, C. Del Negro, N. Pergola, V. Tramutoli, Hot spot detection and effusion rate estimation using satellite data to drive lava flow simulations,*Use of Remote Sensing Techniques for Monitoring Volcanoes and Seismogenic Areas, USEReST*, (2008).
9. R. Wright, L. Flynn, , H. Garbeil, A. Harris, E. Pilger, Automated volcanic eruption detection using MODIS. *Remote Sensing of Environment*,**82**, (2002) pp 135-155.